

1-1-1959

# Spectral study of the attenuation of gamma radiation

Jack Jack  
*Iowa State University*

Follow this and additional works at: <https://lib.dr.iastate.edu/rtd>

 Part of the [Engineering Commons](#)

## Recommended Citation

Jack, Jack, "Spectral study of the attenuation of gamma radiation" (1959). *Retrospective Theses and Dissertations*. 18052.  
<https://lib.dr.iastate.edu/rtd/18052>

This Thesis is brought to you for free and open access by the Iowa State University Capstones, Theses and Dissertations at Iowa State University Digital Repository. It has been accepted for inclusion in Retrospective Theses and Dissertations by an authorized administrator of Iowa State University Digital Repository. For more information, please contact [digirep@iastate.edu](mailto:digirep@iastate.edu).

SPECTRAL STUDY OF THE ATTENUATION  
OF GAMMA RADIATION

by

Jack Cowden

A Thesis Submitted to the  
Graduate Faculty in Partial Fulfillment of  
The Requirements for the Degree of  
MASTER OF SCIENCE

Major Subject: Nuclear Engineering

Approved:

Signatures have been redacted for privacy

Director of Major Work

Head of Major Department

Dean of Graduate Studies

Iowa State College

Ames, Iowa

1959



## TABLE OF CONTENTS

	Page
I. INTRODUCTION	1
II. REVIEW OF THE LITERATURE AND THEORY	3
A. General	3
B. Photoelectric Effect	3
C. Compton Scattering	5
D. Pair Production	6
E. Secondary Interaction Processes	7
F. Gamma Ray Absorption Coefficients	7
G. Methods of Calculating Gamma Ray Attenuation	9
III. EQUIPMENT AND PROCEDURE	12
A. Source	12
B. Absorbers	15
C. Detector	15
D. Spectrometer	16
E. Scaler	18
F. Method of Obtaining Data	18
IV. RESULTS AND DISCUSSION	20
A. General Characteristics of the Spectrograms	20
B. Mass Absorption Coefficient	51
C. Energy Buildup Factor	54
V. CONCLUSIONS	60
VI. LIST OF REFERENCES	61
VII. ACKNOWLEDGMENTS	63



## I. INTRODUCTION

In the past ten years, a tremendous amount of work has gone into the investigation of the attenuation of gamma radiation. The problem of gamma ray attenuation would be relatively simple if it were merely an absorptive reaction. However, it is complicated greatly by the energy dependence and by the variety of interactions of gamma rays with matter. Because of the different types of interactions, the attenuation of gamma rays does not lend itself particularly well to experimental determinations and the more detailed and exact results have been determined theoretically.

With the advent of improved counting techniques subsequent to 1947, it has been possible to obtain more accurate experimental results. However, most of the experiments have been performed using a highly collimated beam of monoenergetic gamma rays and recording the half thickness, or absorption coefficients, of the absorbing material with regard to the total amount of electromagnetic radiation issuing from the material. Due to the various interaction processes, the electromagnetic radiation coming from the absorber covers the entire energy range from the energy of the initial gamma ray through the x-ray region.

The variation of the energy spectrum of gamma radiation with increasing absorber thickness is of particular interest since this variation is not constant over the energy range.



With the development of improved gamma ray scintillation crystals, photo multiplier tubes, and recording spectrometers, it is possible to obtain a rather accurate gamma ray energy spectrum using a fairly low intensity source of gamma radiation.

Since gamma ray sources are not collimated in normal use, and since there is some debate as to the degree of collimation that can actually be obtained, it was decided not to collimate the source in this investigation. This idea led to a rather simple experimental setup closely approximating a scintillation detector being placed against the outside of a radiation shield. Lead was chosen as the absorbing material, since it is the primary material used in gamma ray shielding.

If the variations in the energy spectrum with absorber thickness, using this setup, could be correlated with existing theory, it would provide a relatively simple experimental method of determining information on the attenuation of gamma radiation.



## II. REVIEW OF THE LITERATURE AND THEORY

Volumes of literature have been published on interactions of gamma rays with matter. No attempt was made to read through all of this material. Only a few of the more accessible and acceptable articles, dealing with the various aspects of the problem, were chosen for review.

It would be rather pointless to attempt to cover the detailed theory of the various gamma ray interactions. References to the detailed theory will be given and some of the more important equations and results will be shown.

### A. General

There are several good references on the fundamentals of gamma ray interaction processes. For basic understanding Fano (1), Friedlander and Kennedy (3), Kaplan (11), and Segre (19) present a comparatively simple approach to the overall problem. Heitler (6) gives a broader treatment of the problem but is more difficult to follow. One of the latest general works on the attenuation of gamma rays by Goldstein (4) contains excellent material in all phases of the problem: including primary and secondary effects, recent mass absorption coefficients, and some methods of calculation.

### B. Photoelectric Effect

In the photoelectric process the incident photon trans-



fers all of its energy to one of the atomic electrons, ejecting it with an energy equal to the energy of the incident photon less the ionization energy of the electron. Therefore, in order for the process to occur, the energy of the incident photon must be greater than the binding energy of the electron. Since the binding energy of the electrons is small for low  $Z$  elements and increases approximately as  $Z^2$ , the photoelectric effect is much more important in the higher  $Z$  elements. When the electron is ejected from its shell in the atom, an electron from the next outer shell drops into its place and a photon is emitted with energy equal to the difference in binding energy of the two electron shells.

When photon energies are large compared to the ionization energy, the electron appears lightly bound and the photoelectric process becomes less probable. Heitler (6) shows the quantum mechanical derivation of formulas for the probability that a photon of a particular energy will undergo photoelectric absorption. Kaplan (11) gives the simplified formula for the photoelectric cross section per atom

$$a\sigma = \beta_0 Z^5 (1/137)^4 \sqrt{2} (m_0 c^2 / h\nu)^{7/2}, \quad (1)$$

where  $h\nu$  is the energy of the incident photon,  $m_0 c^2$  is the rest energy of the electron,  $Z$  is the atomic number of the absorbing material, and  $\beta_0$  is the Thompson scattering unit

$$\beta_0 = 8\pi/3 (e^2/m_0 c^2)^2 = 0.665 \text{ barns} \quad (2)$$



The values of  $\sigma_a$  obtained from this formula are only accurate for photon energies in the neighborhood of 0.5 Mev and more rigorous formulas must be used for energies differing appreciably from this value.

### C. Compton Scattering

The Compton effect is the scattering of photons by free electrons. The main source of difficulty in the calculation of gamma ray attenuation is caused by the change in direction and energy of the incident photons in this scattering process. Kaplan (11) gives the energy of a photon scattered at a given angle;

$$h\nu = \frac{h\nu_0}{1 + \frac{h\nu_0}{m_0c^2}(1-\cos\theta)}, \quad (3)$$

or in terms of electron rest mass energy,

$$E = \frac{E_0}{1 + \frac{E_0}{m_0c^2}(1-\cos\theta)}, \quad (4)$$

The quantum mechanical development of the Klein Nishina formula for the probability that Compton scattering will occur is shown by Heitler (6). The equation for total scattering cross section per electron is

$$\sigma_c(E) = \frac{3}{4}\sigma_0 \left\{ \frac{1 + E_0}{E_0^3} \left[ \frac{2E_0(1 + E_0)}{1 + 2E_0} - \ln(1 + 2E_0) \right] + \frac{1}{2E_0} \ln(1 + 2E_0) - \frac{1 + 3E_0}{(1 + 2E_0)^2} \right\}, \quad (5)$$



where  $E_0$  is in electron rest mass units and  $\beta_0$  is given by Equation 2. The differential cross section for scattering by a given angle, per unit solid angle, is given by

$$\sigma(\theta)d\Omega = \frac{3}{16} \frac{E^2}{E_0^2} (E_0/E + E/E_0 - \sin^2\theta) d\Omega . \quad (6)$$

Latter and Kahn (12) have compiled tables for the values of the differential cross section and Nelms (16) made an extensive set of graphs of Compton energy angle relationship and the differential cross sections for various scattering angles and initial photon energies.

From Equation 5, it can be seen that the total scattering cross section per electron is independent of  $Z$  and therefore the cross section per atom varies as  $Z$ . It can also be shown from this equation that the total scattering cross section increases with increasing photon energies.

#### D. Pair Production

In pair production the entire energy of the incident photon is transformed into the creation of an electron - positron pair. The kinetic energy of the pair is equal to the energy of the incident photon minus twice the rest mass of an electron. Therefore, the threshold for pair production is  $2m_0c^2$  or 1.022 Mev. Segre (19) has a good development of this process, showing the increase in the effect with  $Z$  and energy.



Since the energy of the source used in this investigation was below the threshold energy, the effect of pair production could be neglected.

### E. Secondary Interaction Processes

There are several secondary processes of photon interaction with matter. These are coherent electron scattering, annihilation radiation, fluorescence radiation, bremsstrahlung, Thomson scattering from the nucleus, potential scattering, coherent molecular or crystal scattering, nuclear interaction, and radiative corrections to lower order processes. Goldstein (4) discusses each of these processes and shows why they can be neglected for actual calculations of gamma ray attenuation.

### F. Gamma Ray Absorption Coefficients

If a beam of photons of flux density  $I$  strikes an absorber which has thickness  $x$ ,  $n$  number of atoms per unit volume, and a collision cross section of  $\sigma$ , then the number of collisions made in a path length  $dx$  by photons passing in unit time through unit cross sectional area of the beam is  $I \sigma n dx$ . Using the macroscopic absorption coefficient  $\mu$ , equal to  $n \sigma$ , this value is  $I \mu dx$ . If the collisions are purely absorptive, this number of collisions must be equal to the decrease in the flux density  $I$  over the distance  $dx$ :



$$-dI = I \mu dx \quad (7)$$

The solution to this simple differential equation is the well known absorption law

$$I = I_0 e^{-\mu x} \quad (8)$$

Since the gamma ray interaction processes are not completely absorptive, Equation 7 does not give the actual decrease in flux density. Therefore Equation 8 does not describe the attenuation of the total beam, but gives the flux density of those photons which survive without having made any collisions.

The total photon cross section is the sum of the cross sections for photoelectric effect, Compton scattering and pair production:

$$\sigma = \sigma_{PE} + \sigma_C + \sigma_{PP} \quad (9)$$

This total cross section is normally expressed as the mass absorption coefficient,  $\mu$ , in units of  $\text{cm}^2/\text{g}$ . Numerous tables of absorption coefficients have been made, based in varying proportions on calculations and measurements with narrow beam geometry. Latter and Kahn (12) made an extensive compilation in 1949. The compilation made by White (22) is one of the most recent and is believed to be accurate within 2 per cent.



### G. Methods of Calculating Gamma Ray Attenuation

In order to calculate the attenuation of gamma radiation it is necessary to know how many photons are going in what direction with what energy at any point. This is given by a flux density function of position, energy and direction,  $N(\vec{r}, E, \vec{\Omega})$ . This function is defined so that  $N(\vec{r}, E, \vec{\Omega}) dE d\Omega$  gives the number of photons at  $\vec{r}$ , with energy  $E$  in range  $dE$ , going in the direction specified by the unit vector,  $\vec{\Omega}$ , within the element of solid angle  $d\Omega$ , which cross in unit time a unit differential element of area whose normal is in the direction  $\vec{\Omega}$ . This value of  $N$  is normally called the angular number flux. Corresponding is the angular energy flux,  $I(\vec{r}, E, \vec{\Omega})$  which refers to the energy carried by the photons rather than to their number. This angular energy flux is equal to  $EN$ .

Goldstein and Wilkins (5) show the derivation of the equation for the transport of gamma rays in terms of  $I$ :

$$\nabla \cdot \vec{\Omega} I + \mu I = \iint I(\vec{r}, E', \vec{\Omega}') \sigma(\vec{\Omega}' \rightarrow \vec{\Omega}, E' \rightarrow E) \frac{E dE'}{E'} d\Omega' + S(\vec{r}, E, \vec{\Omega}), \quad (10)$$

where  $\sigma(\vec{\Omega}' \rightarrow \vec{\Omega}, E' \rightarrow E)$  is the differential cross section for scattering from the direction  $\vec{\Omega}'$  to  $\vec{\Omega}$  and from the energy  $E'$  to  $E$ , and  $S(\vec{r}, E, \vec{\Omega})$  is the energy source function.

The complicated form of Equation 10 insures that any accurate method of solving the transport equation will involve



extensive computations. Welton (21) reviewed some of the methods that have been used up to 1955. Fano and Nelms (2) developed a simplified solution in 1957, but it is only applicable to photons of energy less than 0.5 Mev and fairly low Z absorbers. At present only three successful methods have been developed.

The method of successive scatterings uses the calculation of the unscattered flux to obtain the collision density for the first scattering. By treating the scattered photons as new sources, the flux of singly scattered photons can be found. This process can be repeated until all photons making contributions to the flux are included. After the first scattering this procedure becomes quite involved. Peebles (17) and Peebles and Plesset (18) have carried this method the farthest and give results obtained for lead and iron slabs.

The Monte Carlo technique consists of theoretically tracing the life history of a large number of photons. Each step in the history is chosen at random from the known probability distribution for the given event. Meyer (14) has brought together a number of papers on the Monte Carlo technique including some results of its application to several shielding problems.

The method of moments was developed by Spencer and Fano (20) in 1951. It consists primarily of expanding the angular flux in terms of Legendre polynomials and integrating over

all solid angles. Goldstein and Wilkins (5) have applied this method to an extensive program of gamma ray attenuation calculations with excellent results.



### III. EQUIPMENT AND PROCEDURE

The equipment used in this investigation and the experimental arrangement are shown in Figure 1. A detailed description of the equipment follows.

#### A. Source

The source chosen for this experiment was of cesium-barium 137. This isotope pair emits a monoenergetic gamma ray with an energy of 0.662 Mev due to the decay schemes



and

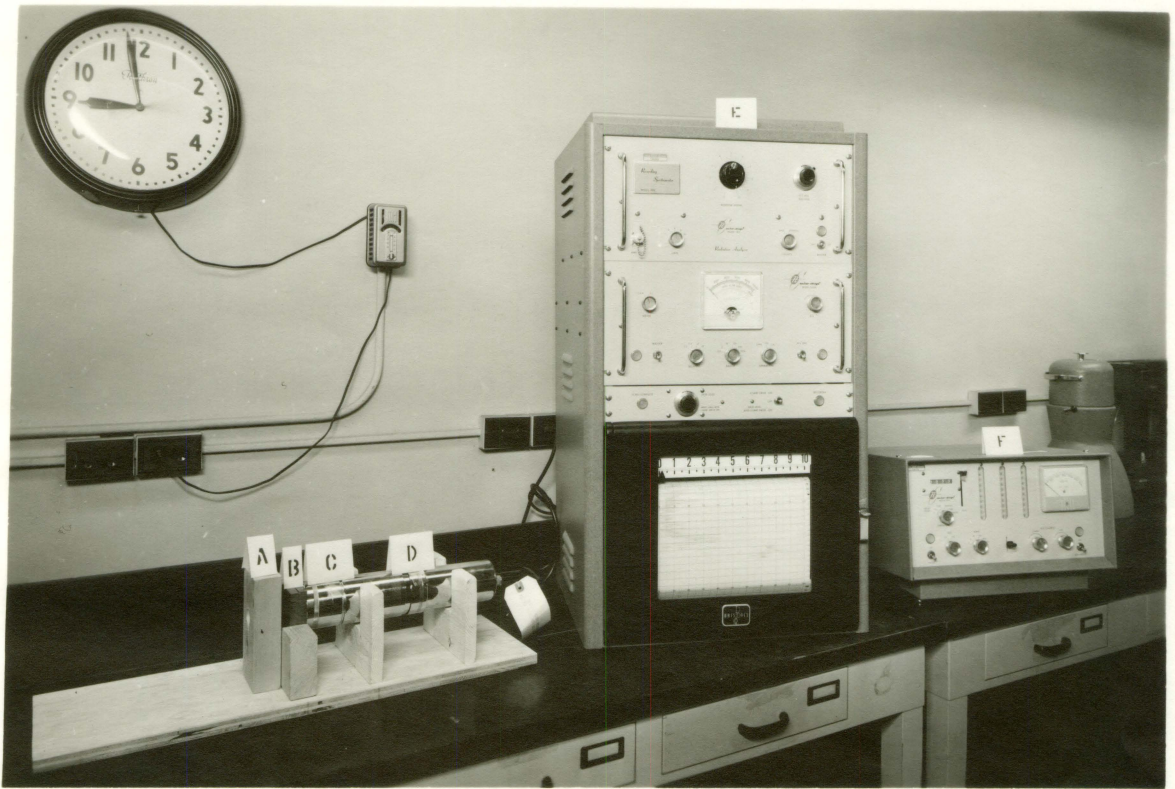


Due to the long half life, the source remained essentially constant over the period of the investigation. The source consisted of a thin layer of cesium, one inch in diameter, on an aluminum planchet. The strength of the source was approximately 0.1 millicuries; the exact strength was not important since only relative values were needed in this investigation. The aluminum planchet was mounted over a hole in a wooden stand to minimize scattering. The source was left at a constant distance of one inch from the scintillation crystal.

Figure 1. Experimental equipment

- A. Source
- B. Lead absorber
- C. Crystal and adapter
- D. Basic probe
- E. Spectrometer
- F. Scaler







### B. Absorbers

Lead was used as the absorbing material. It was in the form of three inch squares of varying thicknesses. The thickness of these lead plates was measured in grams per square centimeter; the maximum thickness being  $14.7 \text{ g/cm}^2$  or about 1/2 inch. The absorber in use was held against the face of the scintillation crystal by a wooden bracket.

### C. Detector

The detector used in this experiment was the Nuclear-Chicago Model DS5 Versatile Scintillation Counter which was designed for operation with scalars, rate meters, or differential pulse-height analyzers. This detector consists of three parts; the basic probe, a crystal adapter, and the scintillation crystal.

The basic probe is made up of the housing, inner lead shielding, photo multiplier tube, preamplifier circuit, and the attached cables. The photo multiplier tube is the RCA type 665. Morton (15) gives a good discussion of the use of this type of tube for scintillation counting.

The AX6S crystal adapter used for the well type crystal consists of the housing which screws on to the DS5 basic probe, a light pipe, and an internal lead shielding ring.

The scintillation crystal used was the XT2W0 well-type crystal. This is a thallium activated sodium iodide crystal



hermetically sealed in a 1/32 inch aluminum can. The dimensions of the crystal are 1-7/8 inches in diameter by 2-1/4 inches thick with a 21/32 inch diameter well 1-1/2 inches deep. This crystal was primarily designed for use with test tubes and centrifuge tubes. Due to the geometry of the experiment, the well had no effect on the results.

Hofstadter (7, 8), Hofstadter and McIntyre (9) and Jordan and Bell (10), who have done a vast amount of investigation of scintillation materials, recommend the thallium activated sodium iodide crystal as the best available for gamma ray detection. They estimate the detection efficiency of this type of crystal to be approximately 45%, depending on geometry. Maeder and Winterstieger (13) used this type of crystal in the investigation of gamma ray spectra with excellent results.

#### D. Spectrometer

The scintillation detector was connected to a Nuclear-Chicago Model 1820 Recording Spectrometer. This is a single channel differential pulse-height analyzer which automatically scans the pulse height spectrum and graphically records the input pulse rate versus pulse height on a paper strip chart. This instrument consists of a radiation analyzer, a count rate meter, and a recorder.

The pulses from the scintillation detector are fed into a linear amplifier in the radiation analyzer and then into



both of two amplitude discriminating circuits. The base level discriminator sets the voltage level below which all pulses are rejected. The base level can be adjusted from 1 to 100 volts by the base level control. From the known pulse height of a source, the base level can be calibrated by means of a high voltage control. The upper discriminator is referenced to the base level discriminator. A voltage of from 0 to 10 volts above base level voltage can be set by means of the window width control. Both of these discriminators feed into an anticoincidence circuit which rejects pulses received simultaneously from both discriminators and passes only those pulses received alone from the base level discriminator. For operation as a recording spectrometer, scanning of the radiation energy range is produced by a linear sweep of the base level discriminator voltage. This is accomplished by motor driving the base level control at a standard rate of one-half hour per complete scan.

The selected pulses from the radiation analyzer are fed into the count rate unit which provides a controllable amount of integration. The output signal, which is proportional to the number of pulses per minute, is fed to the visual meter on the front of the spectrometer and also to the chart recorder.

The recorder is used to obtain a large linear presentation of the radiation spectrograms. The input signal is fed

into a self balancing d-c potentiometer which drives the recording pen. The count rate is then indicated by pen displacement, and the radiation energy is represented by the distance along the time axis of the chart.

#### E. Scaler

Due to the fluctuation of the count rate meter, the base level voltage can be more accurately calibrated by attaching a scaler to the radiation analyzer. A standard Nuclear-Chicago Model 151A Scaler was used for this purpose.

#### F. Method of Obtaining Data

The apparatus was arranged on a table as shown in Figure 1. The table was placed in the center of the room to minimize scattering from the walls. After allowing the equipment time to warm up, the source was placed in position, and the spectrometer was calibrated for 662 kev by adjusting the high voltage until the maximum count rate was obtained on the scaler. For all runs the spectrometer was set with a gain of 4:1, a count rate range of 30,000 counts per minute, a window width of one volt, and a time constant of two seconds.

With the spectrometer adjusted, the base level control was set at maximum pulse height, corresponding to 1 Mev. A lead absorber was then placed in the holder and the chart and base level drive turned on.



After the first few sample runs, it became apparent that the spectrometer was extremely sensitive to small line voltage fluctuations and small temperature changes. The fluctuation in line voltage was corrected by the use of a voltage regulator. By allowing a warm up period of at least an hour and a half, the temperature of the spectrometer was stabilized. However, small changes in room temperature were still enough to cause an appreciable change in the peak pulse height. Therefore, it was necessary to calibrate the spectrometer before and after every run, and discard the results if it was found that the peak pulse height had shifted during the run.

The data were obtained in the form of radiation spectrograms at varying absorber thicknesses.



#### IV. RESULTS AND DISCUSSION

##### A. General Characteristics of the Spectrograms

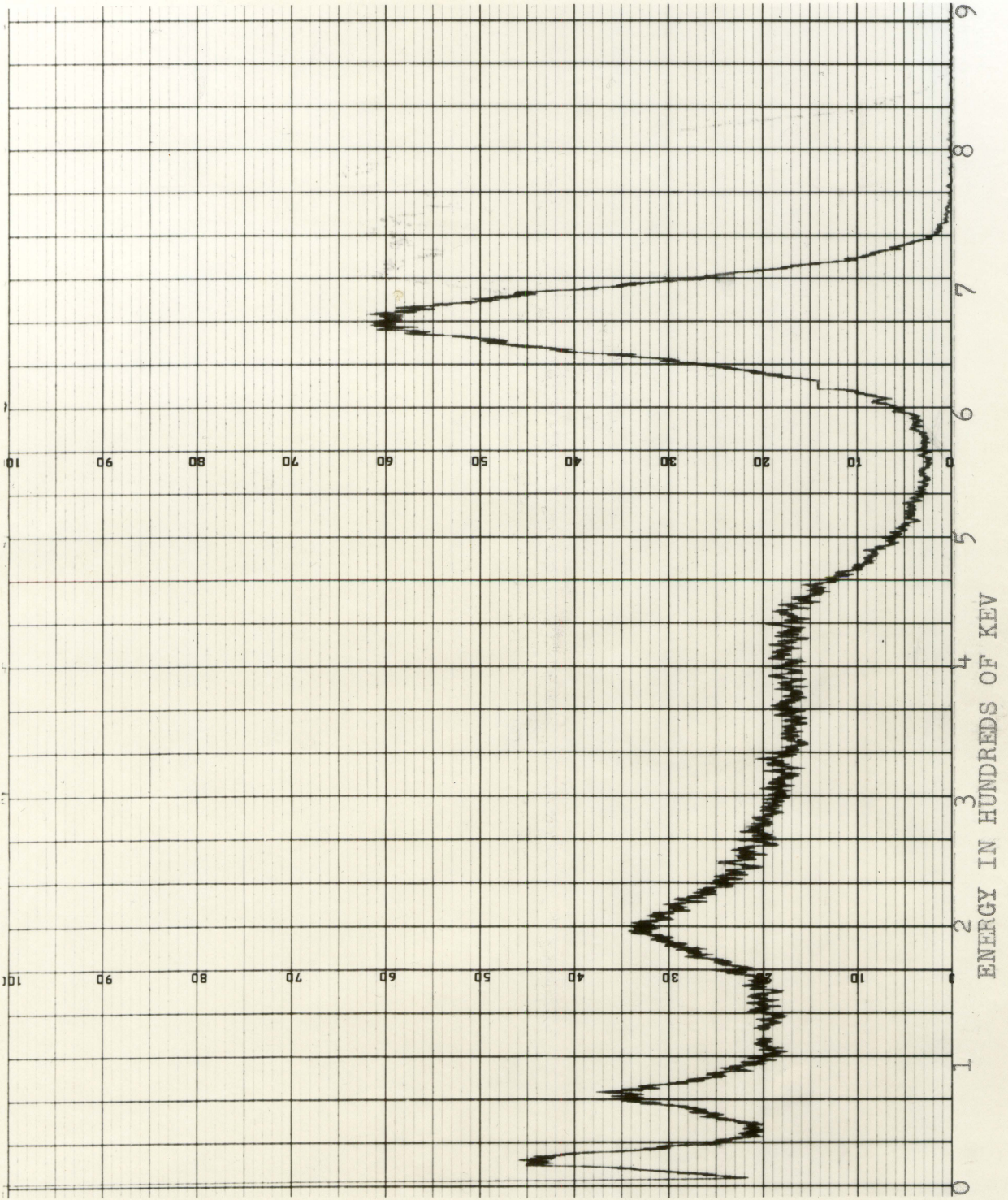
Some of the spectrograms obtained in this investigation are shown in Figures 2 through 11. The changes in the amount and energy of the penetrating radiation with variations of absorber thickness are shown graphically in these figures. A great amount of the scattered radiation appearing at the lower energy regions in Figure 1, with no absorber, is due to the lead shielding in the scintillation detector. Since about half of the source radiation incident on the scintillation crystal passes through undetected, it will not be absorbed in the crystal. The lead liner will scatter some of this undetected portion back into the crystal causing lower energy scintillations. The effect of this internally scattered radiation will be discussed along with the effects of the absorber at different energy ranges of the spectrograms.

The predominant peak on all of the spectrograms, at 662 kev, is a measure of the number of unabsorbed and unscattered photons reaching the detector. The decrease in this peak with lead absorbers in place is a measure of the number of photons which are both scattered and absorbed.

Proceeding down the energy scale, the effect of Compton scattering becomes apparent. In Figure 2, with no absorber,

Figure 2. Gamma ray energy spectrum of the cesium source  
from 0 to 900 kev, without absorber





COUNTS PER MINUTE DIVIDED BY 300

ENERGY IN HUNDREDS OF KEV



Figure 3. Gamma ray energy spectrum of the cesium source from 0 to 900 kev, with a 0.92 g/cm<sup>2</sup> lead absorber

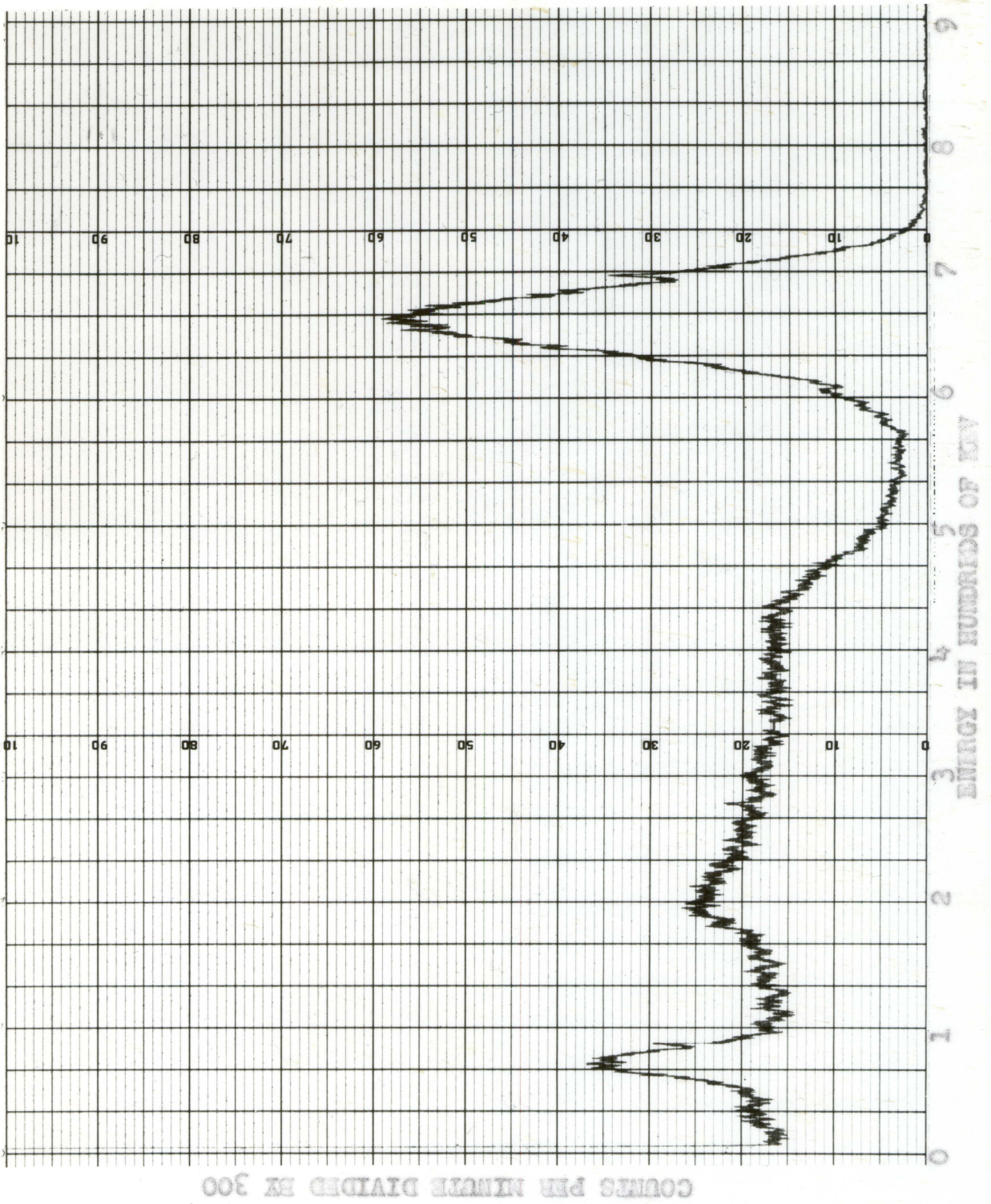




Figure 4. Gamma ray energy spectrum of the cesium source  
from 0 to 900 kev, with a 1.82 g/cm<sup>2</sup> lead absorber

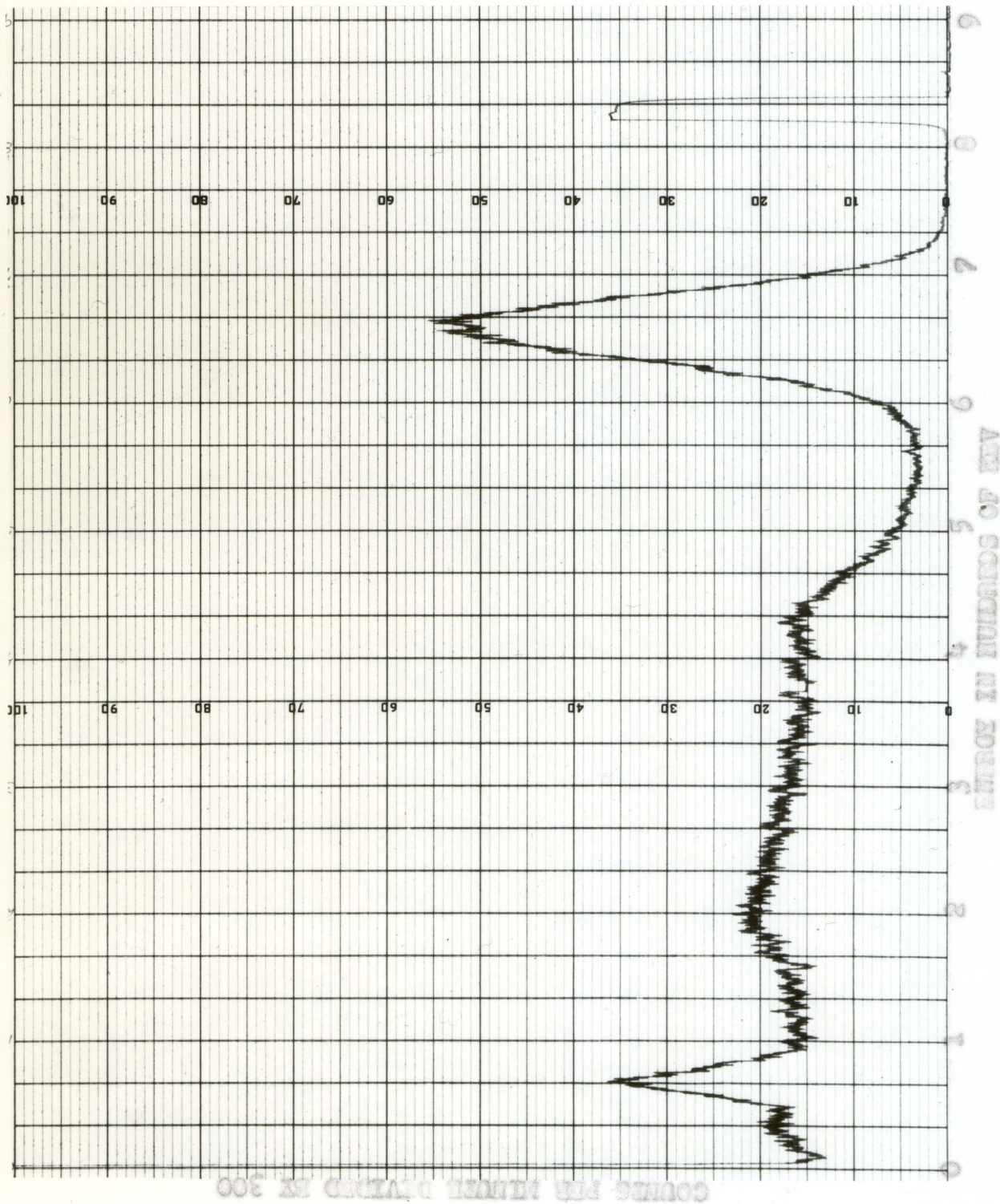




Figure 5. Gamma ray energy spectrum of the cesium source  
from 0 to 900 kev, with a  $2.74 \text{ g/cm}^2$  lead absorber

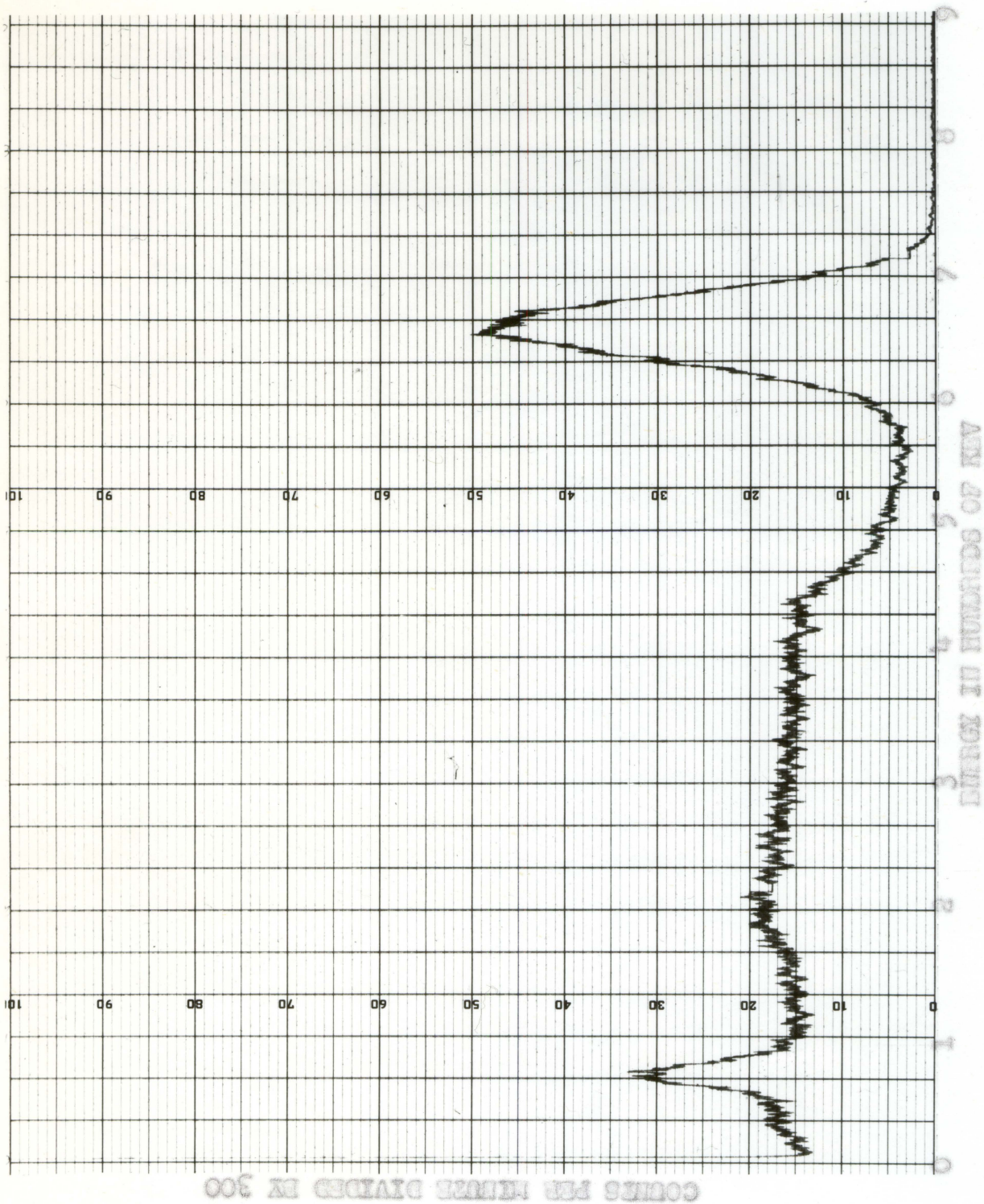




Figure 6. Gamma ray energy spectrum of the cesium source  
from 0 to 900 kev, with a 3.64 g/cm<sup>2</sup> lead absorber



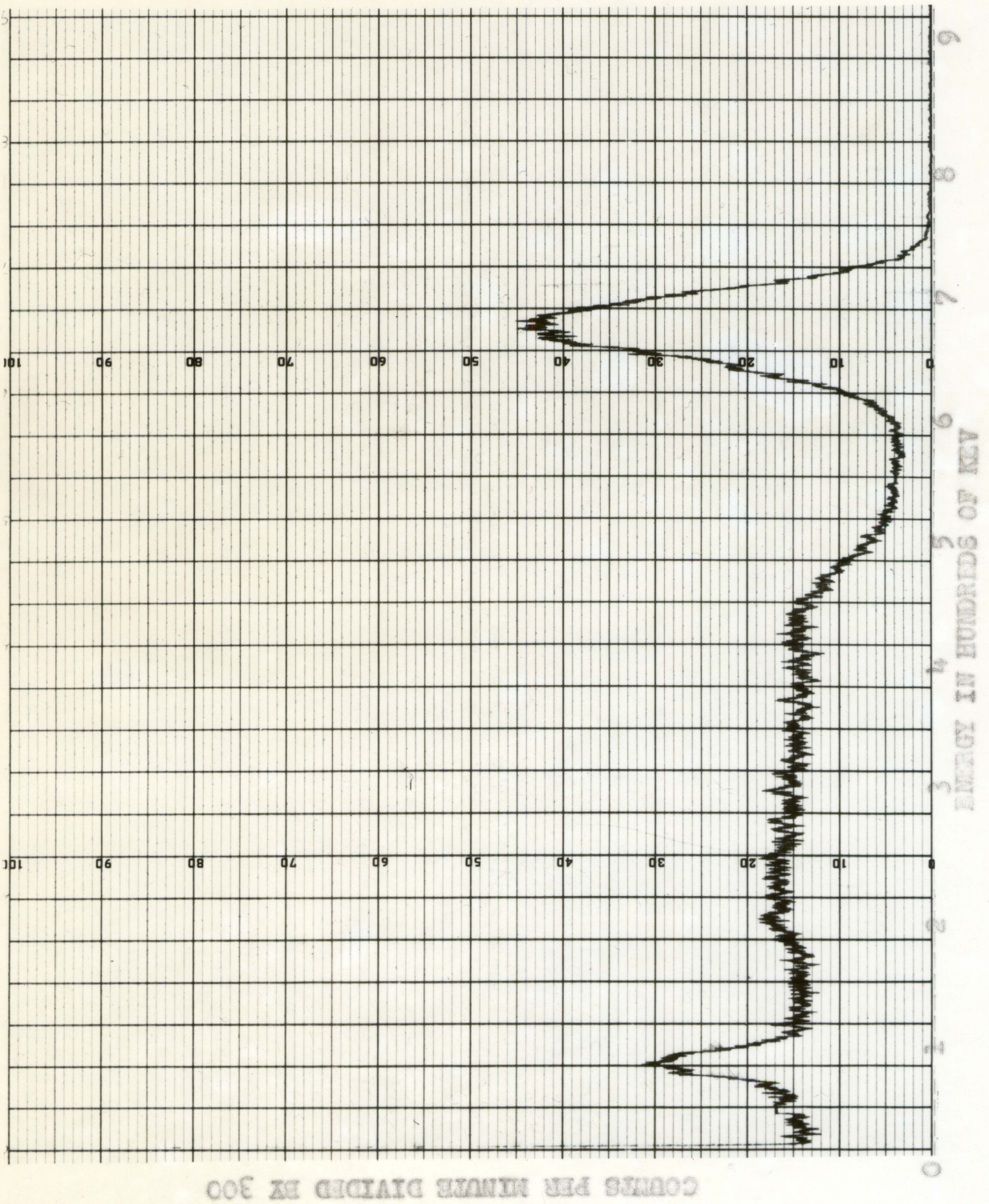




Figure 7. Gamma ray energy spectrum of the cesium source  
from 0 to 900 kev, with a 4.56 g/cm<sup>2</sup> lead absorber



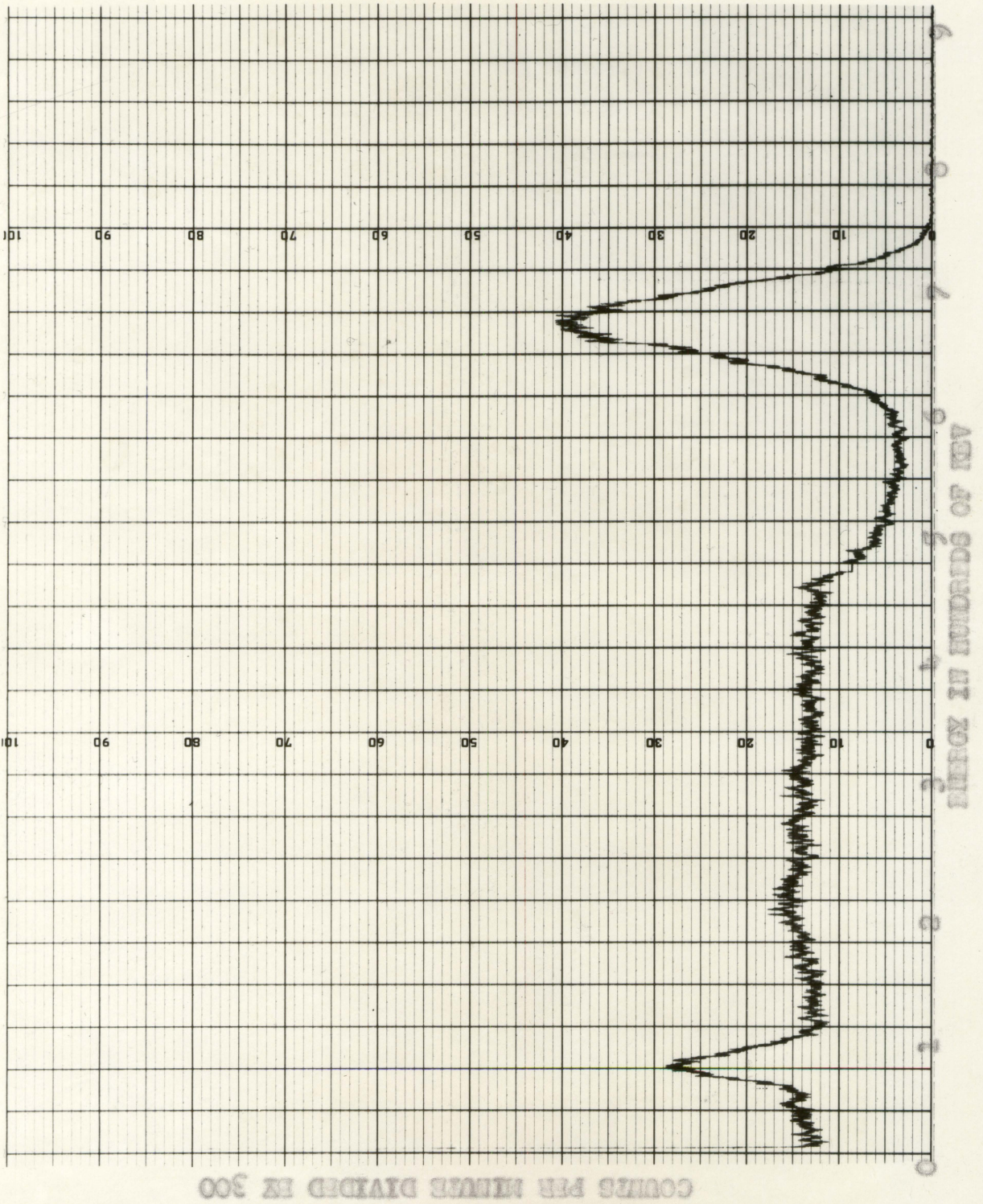




Figure 8. Gamma ray energy spectrum of the cesium source  
from 0 to 900 kev, with a 5.46 g/cm<sup>2</sup> lead absorber

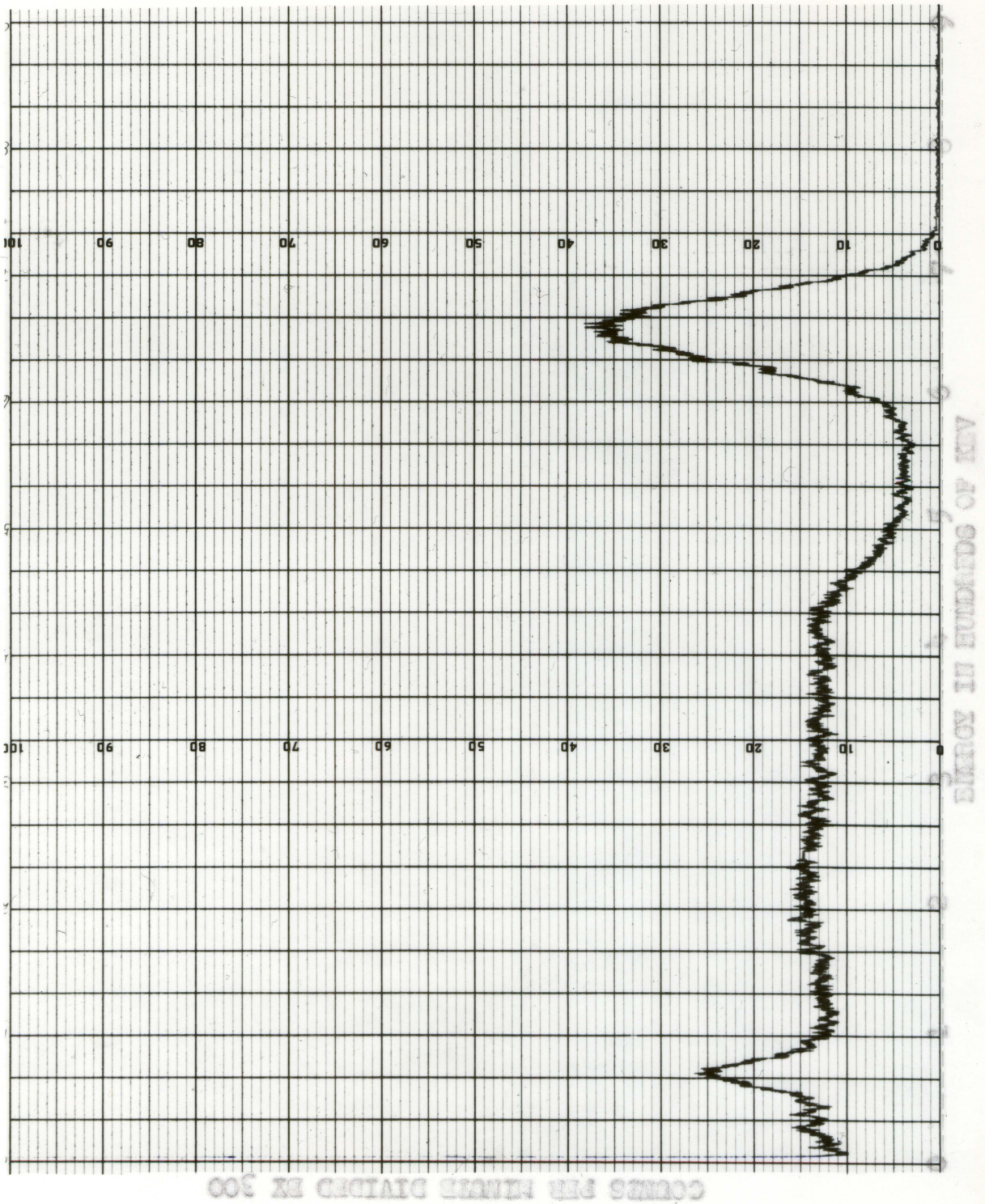




Figure 9. Gamma ray energy spectrum of the cesium source  
from 0 to 900 kev, with 6.38 g/cm<sup>2</sup> lead absorber



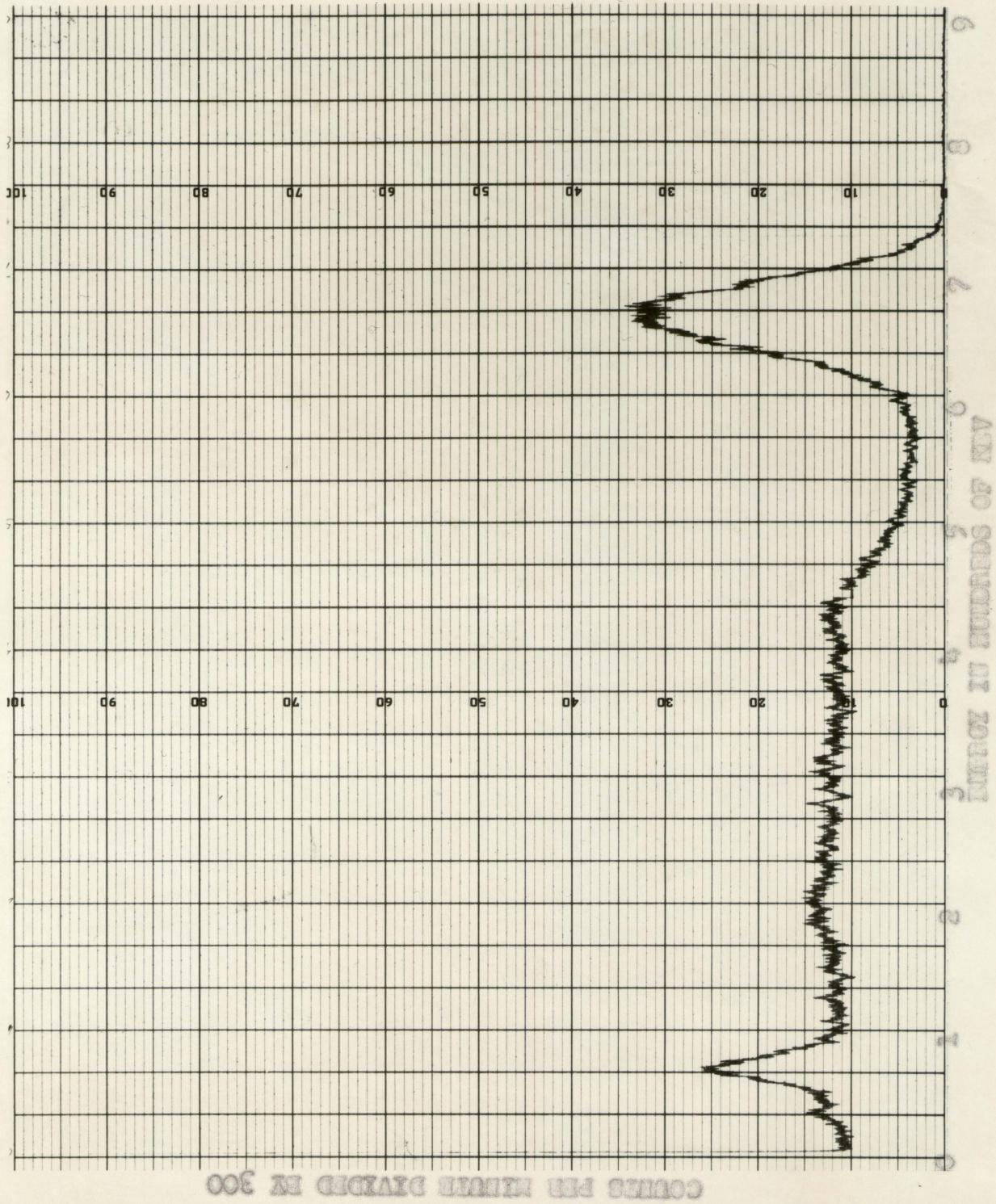
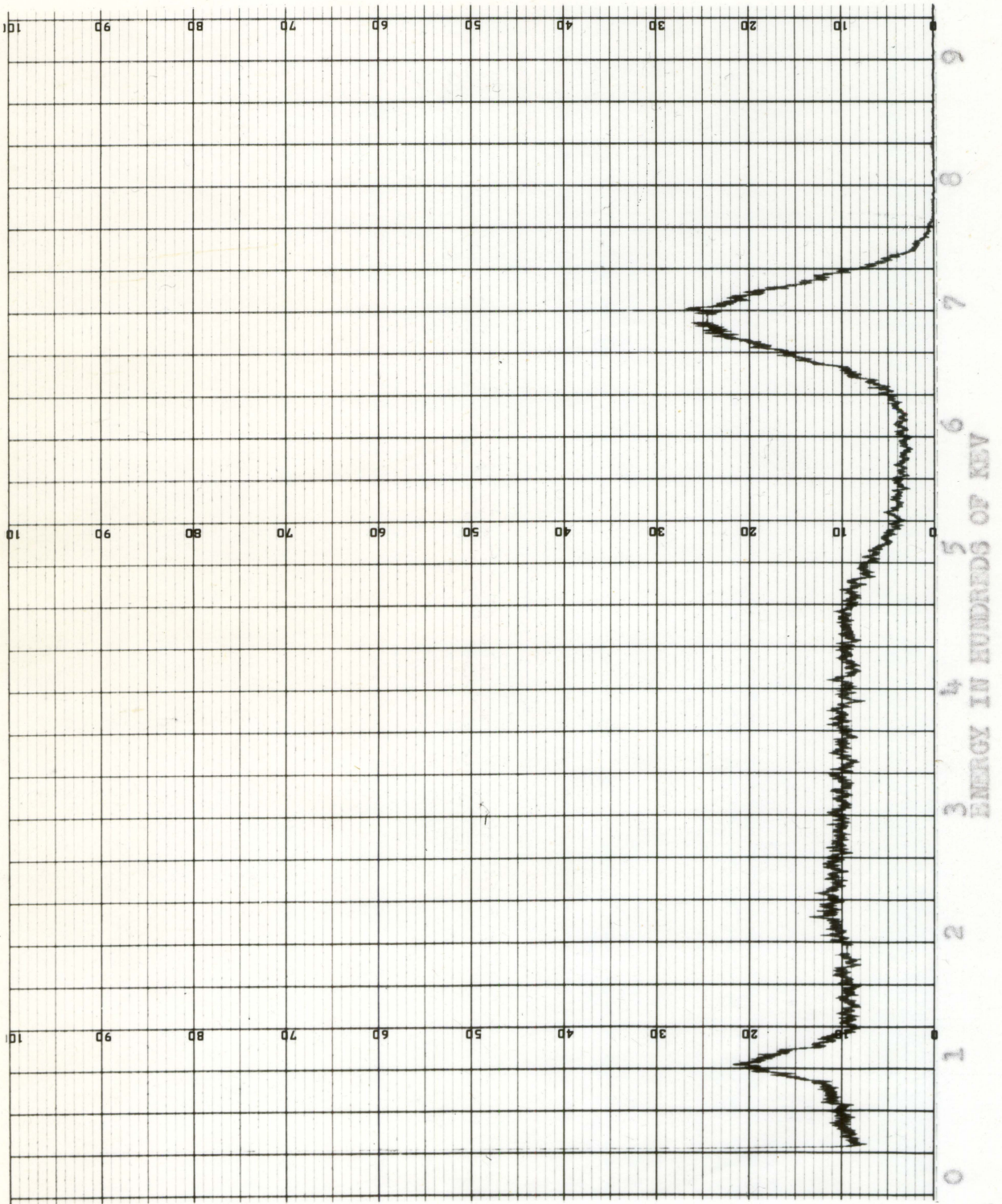




Figure 10. Gamma ray energy spectrum of the cesium source  
from 0 to 900 kev, with a  $9.10 \text{ g/cm}^2$  lead absorber

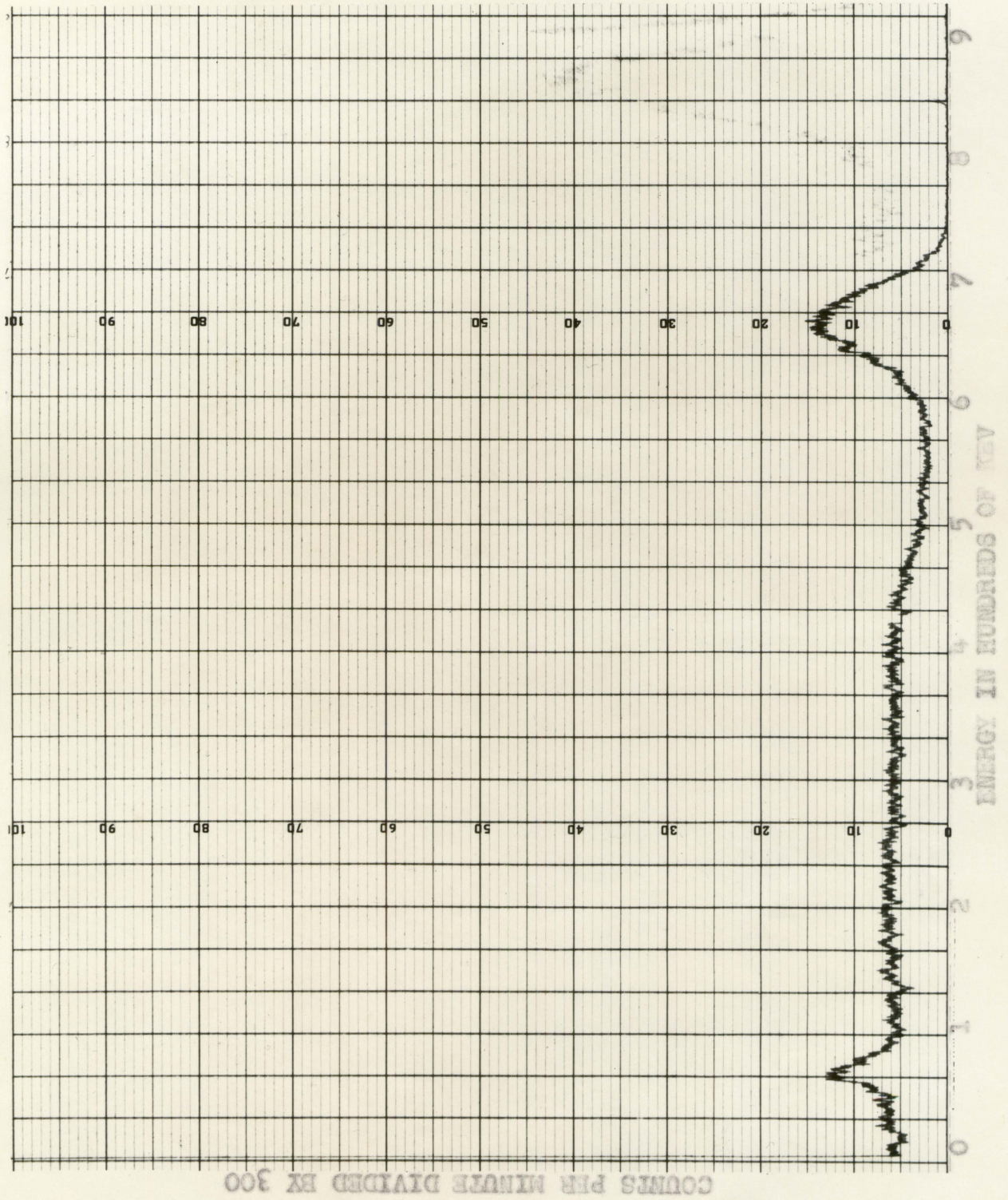


COUNTS PER MINUTE DIVIDED BY 300



Figure 11. Gamma ray energy spectrum of the cesium source  
from 0 to 900 kev, with a 14.70 g/cm<sup>2</sup> lead absorber







this scattering is due to the internal scattering in the detector.

There are two contributions to the internal Compton scattering. The first contribution is from the interaction of the gamma rays with the scintillation crystal. If a photon is scattered in a collision with the iodine in the crystal, the scattered photon may be absorbed in the crystal or it may penetrate on through the crystal. If the scattered photon is absorbed, the detector will register the complete interaction as a single pulse with a height equal to the energy of the incident photon. However, if the scattered photon penetrates through the crystal, the detector will register a single pulse with a height equal to the energy lost by the incident photon in the scattering collision. Since the higher energy photons have a greater tendency to penetrate the crystal without being absorbed, the effect will be more pronounced for collisions at small angles. These low angle collisions cause little energy loss to the photons and the detector will register a greater amount of this type of internal Compton scattering in the lower energy range. With no absorber, this contribution to the internal Compton scattering will vary directly with the peak height of the 662 kev peak.

The second contribution to the internal Compton scattering is due to the liner of the detector. Part of the gamma



rays incident on the scintillation crystal will penetrate the crystal with no interaction. Some of these will be scattered back into the crystal by the liner. Since a photon would have to be scattered at an angle of at least  $90^\circ$  to get back into the crystal, the effect of the internal scattering should appear at an energy corresponding to the energy of a 662 keV photon scattered at  $90^\circ$  and be fairly constant at all lower energies. Using Equation 4, this energy was calculated to be 400 keV, which agrees quite well with the energy where the internal scattering occurs in Figure 2. This internal scattering should vary almost directly with the number of unscattered photons incident on the detector. Therefore the contribution of the internal detector scattering to the spectrographs will vary proportionately as the height of the 662 keV peak. However, with the lead absorbers in place, there is added to the internal scattering a contribution from the scattering occurring in the absorber. This addition can be easily seen by comparing Figure 2 with Figure 11. In Figure 2, the height of the Compton scattering is 28 per cent of the height of the 662 keV peak compared with 43 per cent for Figure 11.

At lower energies, there are other effects which are added to the Compton scattering. These effects appear as peaks on top of the scattering curve on the spectrograms.

Photons will be scattered from the aluminum backing on



the source. In order to reach the detector they must be scattered at approximately  $180^\circ$ . Their energy, calculated from Equation 4, should be 185 kev which agrees closely with the first peak in the scattering region of the spectrograms. In order to reach the detector these back-scattered photons must pass through the absorber; since photons of this energy are more readily absorbed in lead, their contribution decreases rapidly with increasing absorber thickness.

The peak next lower in energy is due to the characteristic K x-ray from photoelectric absorption in lead. The energy of this x-ray is equal to the difference in energy between the K and L shell in lead, having a value of 72 kev. The lead shield in the detector and the lead absorber will both contribute to the photoelectric peak. The internal contribution from the detector will again be closely proportional to the unscattered radiation reaching the detector. The only photoelectric x-rays reaching the detector from the absorber will be due to the photoelectric processes occurring near the surface of the absorber on the detector side, since the x-rays originating away from the surface of the absorbing material will be absorbed by the material. This is confirmed by the slight increase in the photoelectric peak when a thin absorber was used, as shown in Figure 3. Therefore, the absorber contribution to the photoelectric peak is proportional to the amount of radiation penetrating the absorber.



material.

The lowest energy peak on the spectrograms only occurred when there was no absorber, as shown in Figure 2. This is due to the fact that this x-ray originated in the source. It is the characteristic barium K x-ray, caused by the photoelectric process occurring in the barium, which was formed during the disintegration of the cesium source. Due to its low energy of 31 kev, this x-ray is absorbed in small thicknesses of lead and did not appear when any of the absorbers were in place.

Two methods were used in determining the variation of gamma ray flux with absorber thickness. The first method dealt with number flux and the second with energy flux or intensity.

If  $N(E)$  is the number of photons of a particular energy which enter the detector crystal, then the variation in  $N(E)$  with increasing absorber thickness can be determined by measuring the count rate at a particular energy point on each of the spectrograms. Table 1 shows values of the count rate versus absorber thickness for several energy points.

Figure 12 is a semi-logarithmic plot of the values shown in Table 1. The fact that the resulting curves tend to be straight lines indicates an exponential variation of count rate with absorber thickness, or that

$$N(E) = N_0(E)e^{-\mu x} . \quad (11)$$



Figure 12. Variation of count rate with absorber thickness and energy

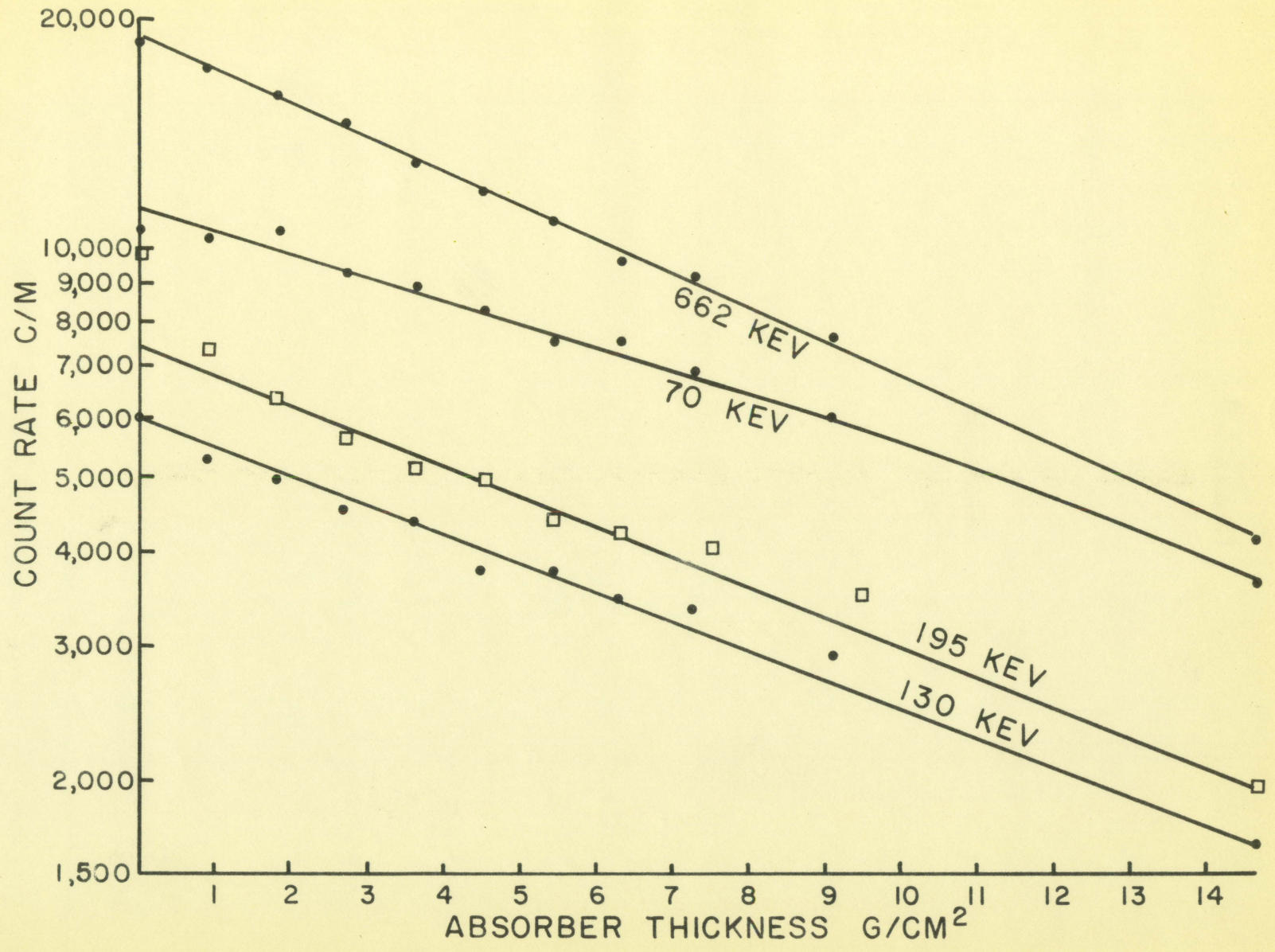




Table 1. Variations of count rate, in counts per minute, with absorber thickness and energy

Absorber thickness g/cm <sup>2</sup>	70 kev	130 kev	195 kev	662 kev
0	10500	6000	9800	18800
0.92	10650	5250	7350	17250
1.82	10500	4950	6300	15900
2.74	9300	4500	5500	14500
3.64	8850	4350	5100	12900
4.56	8250	3750	4950	11850
5.46	7500	3750	4350	10800
6.38	7500	3450	4200	9600
7.28	6900	3380	3900	9200
9.10	6000	2850	3400	7650
14.70	3600	1650	1950	4125

The changes in the slope at the different energy points shows that the value of  $\mu$  is a function of energy.

If  $I(E)$  is the intensity of the photons of a particular energy range which enter the detector crystal, defined such that

$$I(E) = E N(E) , \quad (12)$$

then the variation in  $I(E)$  with increasing absorber thickness can be determined by measuring the area under the spectrogram curves for that particular energy range. Values of area

versus absorber thickness for the unscattered 662 kev peak and the photoelectric peak are shown in Table 2. The values of the areas obtained in this graphical integration were tabulated in square centimeters since only relative values were being considered.

Table 2. Variation of peak areas with absorber thickness

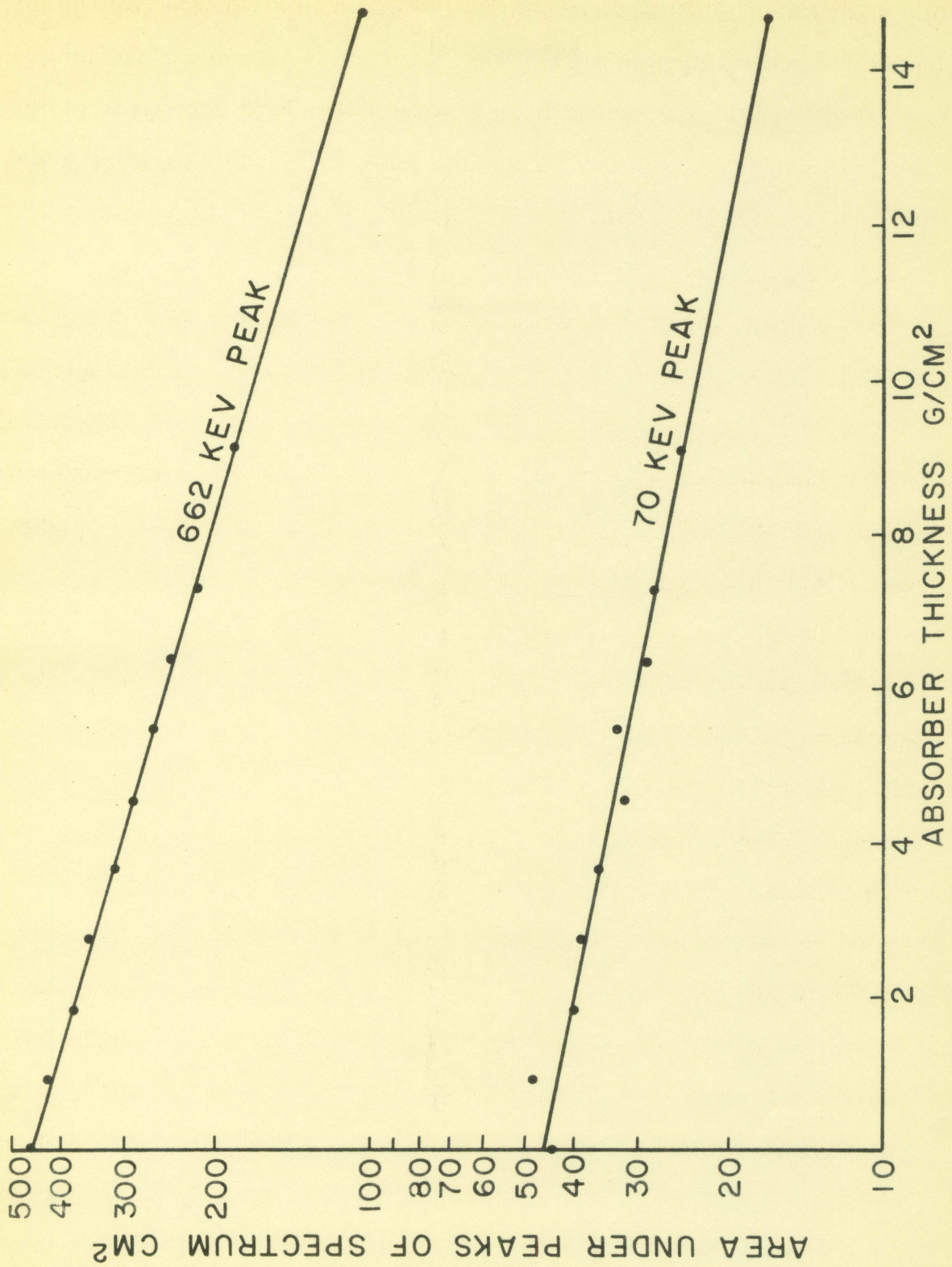
Absorber thickness $g/cm^2$	Area under 662 kev peak $cm^2$	Area under 72 kev peak $cm^2$
0	457	45
0.92	423	48
1.82	380	40
2.74	352	39
3.64	312	36
4.56	289	32
5.46	267	34
6.38	246	29
7.28	219	28
9.10	185	25
14.70	104	17

When these values were plotted on the semi-logarithmic plot shown in Figure 13, the resulting curves were again straight lines, indicating that

$$I(E) = I_0(E) e^{-\mu x} . \quad (13)$$



Figure 13. Variation of peak areas with absorber thickness





Since the slope of the curves in Figure 13 is the same as the slope of the curve in Figure 12 for the same value of energy, it is apparent that the value of  $\mu(E)$  is the same for the variation in both  $N(E)$  and  $I(E)$ .

### B. Mass Absorption Coefficient

In determining gamma ray mass absorption coefficients it has been the practice to calculate or measure the amount of unscattered radiation penetrating a material and give the results in the form of the slope of the unscattered absorption curve for a particular energy. Table 3 shows some values of  $\mu$ , for lead, which were determined by White (22) and are considered to be accurate.

The value of  $\mu$  for a 662 kev gamma ray was calculated to be 0.106 using Equation 1, 5 and 9. Since these equations were simplified, this calculated value was not expected to be exact.

It has been shown that the peak height of the 662 kev peak in the spectrograms is a measure of the unscattered gamma radiation which penetrates the absorber. Therefore, the slope of the 662 kev curve in Figure 12 or Figure 13 should be a direct measure of the gamma ray mass absorption coefficient in lead. The thickness of lead required to reduce the gamma ray intensity to one half the initial value was determined to be  $6.8 \text{ g/cm}^2$ . This gave a value for  $\mu$

Table 3. Gamma ray mass absorption coefficient,  $\mu$ , for lead, in  $\text{cm}^2/\text{g}$  (after G. R. White)

Energy MeV	$\mu$ $\text{cm}^2/\text{g}$
0.04	9.76
0.05	5.19
0.06	3.15
0.08	1.41
0.08823 K edge	1.09
0.08823 K edge	7.42
0.10	5.29
0.15	1.84
0.20	0.896
0.30	0.356
0.40	0.208
0.50	0.145
0.60	0.114
0.80	0.0836
1.00	0.0684

of 0.102.

In order to compare the experimentally determined value of  $\mu$  with accepted values of  $\mu$  for lead, a logarithmic graph of the values from Table 3 was plotted in Figure 14. When the experimental value was plotted on this graph it



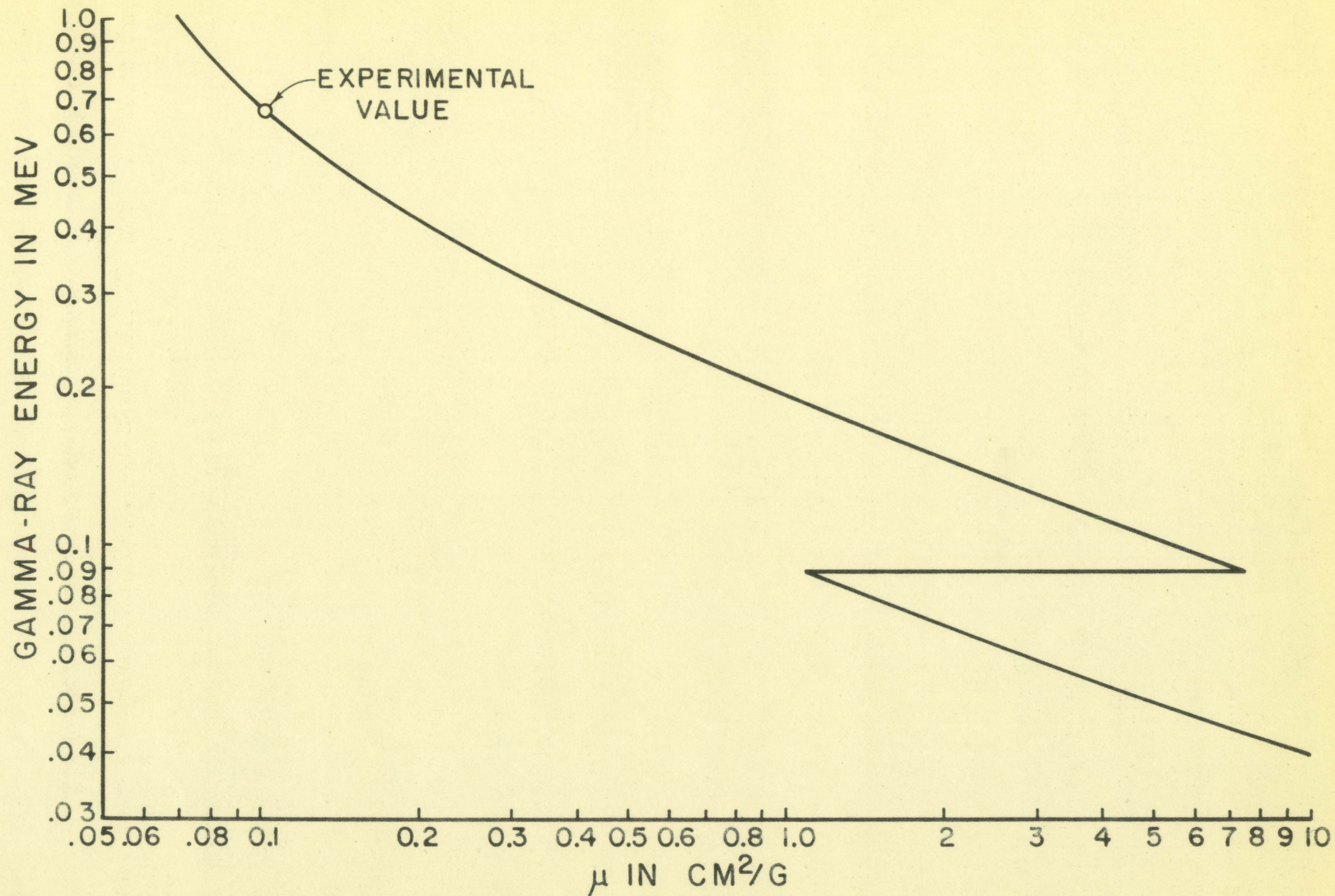


Figure 14. Mass absorption coefficients of gamma rays in lead determined by G. R. White, showing location of experimentally determined value



fell exactly on the curve of accepted values.

### C. Energy Buildup Factor

In calculations of the attenuation of gamma radiation, the results are normally given as buildup factors. This is the factor which, when multiplied by the unscattered contribution, will give the total contribution of the gamma radiation.

In the experimental determination of buildup factors, it has been the usual practice to use two measurements. First, the narrow beam attenuation is found using a highly collimated beam of monoenergetic gamma rays and a collimated detector. Then the broad beam attenuation is found using monoenergetic gamma rays without collimation. The number which must multiply the narrow beam attenuation in order to obtain the broad beam attenuation is the buildup factor.

There are various buildup factors. The number buildup factor  $B_n$  is given by

$$B_n = \frac{\int N dE}{\int N^{\circ} dE}, \quad (14)$$

where the superscript<sup>o</sup> refers to the photons which have not suffered a collision. The corresponding energy buildup factor is given by

$$B_E = \frac{\int I dE}{\int I^{\circ} dE}. \quad (15)$$

Some values of the energy buildup factor in lead which were



calculated by Goldstein and Wilkins (5), are shown in Table 4.

In order to determine the energy buildup factor experimentally it is necessary to determine the values of  $\int I^0 dE$  and  $\int IdE$ . It has been previously shown that  $\int I^0 dE$  for the cesium source can be determined from the area under the 662 kev peak of the spectrograms. However, the value  $\int IdE$  cannot be determined from the total area under the spectrogram curve due to the contribution of the internal effects of the detector. Therefore, in order to determine  $B_E$ , it was necessary to make several assumptions.

It was previously shown that the variation in the contribution of the effects occurring in the lead shield in the detector is approximately the same as the variation of photons of source energy. Therefore, if the total area under the

Table 4. Energy buildup factor,  $B_E$ , in lead [after Goldstein and Wilkins (5)]

$\mu_0 x$	.05 Mev	1.0 Mev
1	1.24	1.37
2	1.39	1.65
4	1.61	2.12
7	1.84	2.71
10	2.04	3.28
15		4.17

spectrogram in Figure 2 is considered as the unscattered contribution of the source photons, then the area of the unscattered contribution in the succeeding spectrograms should vary as the 662 kev peak. This means that

$$A^{\circ} = A_0^{\circ} e^{-\mu_0 x} . \quad (16)$$

There are two major discrepancies in this assumption. The barium K x-ray peak and the 180° back scattering peak do not vary as the unscattered radiation. Since both of these effects appear as peaks on the scattering portion of the spectrogram curves, these discrepancies can be corrected by subtracting the areas of the peaks from the total area under the curve.

Taking the first assumption into account, it can now be assumed that the total area under the spectrogram curves is a measure of the total contribution of the gamma radiation. There is a discrepancy in this assumption due to the internal detector scattering of the scattered gamma radiation from the absorber. However, this is a second order effect and can be neglected for small scattering contributions.

Using these two assumptions, it is now possible to determine the energy buildup factor from the equation,

$$B_E = \frac{\int I dE}{\int I^{\circ} dE} = \frac{A}{A^{\circ}} \quad (17)$$

The experimentally determined values of  $A$ ,  $A^{\circ}$ , and  $B_E$  are



shown in Table 5.

When the calculated values of  $B_E$  from Table 4, and the experimental values of  $B_E$  from Table 5 were plotted versus absorber thickness in Figure 15, the experiment curve ap-

Table 5. Areas under spectrogram curves and experimentally determined values of energy buildup factor in lead

Absorber thickness $\mu/\text{cm}^2$	$\mu_{\text{Co}}x$	A $\text{cm}^2$	$A^0$ $\text{cm}^2$	$B_E$
0	0	150.4	150.4	1.00
0.92	0.0938	141.5	137.5	1.03
1.82	0.185	130.6	124.8	1.05
2.74	0.279	122.5	113.5	1.08
3.64	0.371	113.5	103.5	1.09
4.56	0.465	106.0	94.2	1.13
5.46	0.556	99.5	86.0	1.16
6.38	0.650	92.9	78.3	1.19
7.28	0.742	87.1	71.4	1.22
9.10	0.928	76.7	59.2	1.30
14.70	1.50	45.6	33.4	1.37

peared in the proper location. This indicates that the experimental values of  $B_N$  determined by this method are fairly accurate for absorbers of the thicknesses considered. It is suspected that the neglect of the second order scattering in the detector would cause this method of determina-



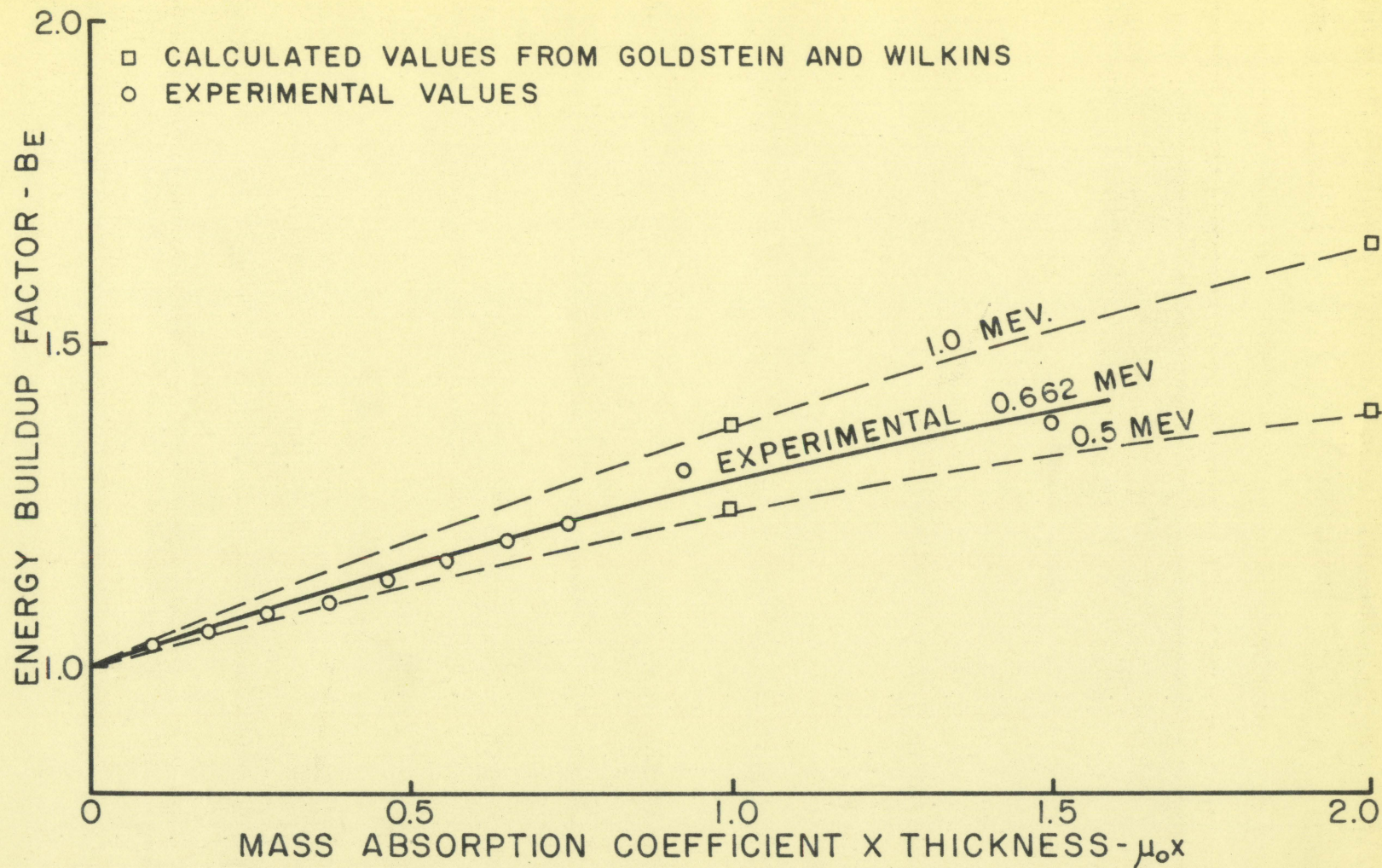


Figure 15. Energy buildup factors, calculated by Goldstein and Wilkins, for lead at 0.5 Mev and 1.0 Mev, along with experimentally determined values at 0.662 Mev



tion to become inaccurate with absorbers of greater thicknesses.

## V. CONCLUSIONS

1. The use of the scintillation detector and the scintillation spectrometer provides a rather simplified method of studying attenuation of gamma radiation.

2. The value of the mass absorption coefficient, obtained by this method, was quite accurate.

3. Values of the energy buildup factor, obtained by this method, appeared to be fairly accurate for the thicknesses of lead which were investigated.



## VI. LIST OF REFERENCES

1. Fano, U. Gamma ray attenuation. *Nucleonics* 11, No. 8: 8-12; and No. 9: 55-61. 1953.
2. \_\_\_\_\_ and Nelms, A. T. An approximate expression for gamma-ray degradation spectra. *J. Research Nat. Bur. Standards* 59: 207-210. 1957.
3. Friedlander, G. and Kennedy, J. W. Nuclear and radio-chemistry. New York, N. Y., John Wiley and Sons, Inc. 1955.
4. Goldstein, H. The attenuation of gamma rays and neutrons in reactor shields. Washington, D. C., U. S. Govt. Print. Off. 1957.
5. \_\_\_\_\_ and Wilkins, J. E., Jr. Calculations of the penetrations of gamma rays. U. S. Atomic Energy Commission Report NYO-3075 [New York Operations Office, AEC]. 1954.
6. Heitler, W. Quantum theory of radiation. 3rd ed. New York, N. Y., Oxford University Press. 1954.
7. Hofstadter, R. The detection of gamma-rays with thallium-activated sodium iodide crystals. *Phys. Rev.* 75: 796-810. 1949.
8. \_\_\_\_\_. Properties of scintillation materials. *Nucleonics* 6, No. 5: 70-73. 1950.
9. \_\_\_\_\_ and McIntyre, J. A. Gamma-ray spectroscopy in crystals of NaI(Tl). *Nucleonics* 7, No. 3: 32-37. 1950.
10. Jordan, W. H. and Bell, P. R. Scintillation counters. *Nucleonics* 5, No. 4: 30-41. 1949.
11. Kaplan, I. Nuclear physics. Cambridge, Mass., Addison-Wesley Publishing Company, Inc. 1955.
12. Latter, R. and Kahn, H. Gamma ray absorption coefficients. *Rand Corp. R-170*. 1949.
13. Maeder, D. and Wintersteiger, V. Quantitative evaluation of gamma-ray spectra from scintillation measurements. *Physica* 18: 1147-1150. 1952.



14. Meyer, H. A. Symposium on Monte Carlo methods. New York, N. Y., John Wiley and Sons, Inc. 1956.
15. Morton, G. A. Photomultipliers for scintillation counting. Radio Corp. Amer. Review 10: 525. 1949.
16. Nelms, A. T. Graphs of the Compton energy angle relationship and the Klein Nishina formula from 10 kev to 500 Mev. Nat. Bur. Standards Circular 542. 1953.
17. Peebles, G. H. Attenuation of gamma rays. J. Applied Phys. 24: 1272-1287 and 1437-1447. 1953.
18. \_\_\_\_\_ and Plesset, M. S. Transmission of gamma-rays through large thicknesses of heavy materials. Phys. Rev. 81: 430-439. 1951.
19. Segre, E. Experimental nuclear physics. Vol. 1. New York, N. Y., John Wiley and Sons, Inc. 1953.
20. Spencer, L. V. and Fano, U. Penetration and diffusion of x-rays. Calculation of spatial distributions by polynomial expansions. J. Research Nat. Bur. Standards 46: 446-456. 1951.
21. Welton, T. A. A review of analytical methods for the calculation of neutron and gamma ray attenuations. U. S. Atomic Energy Commission Report TID-256 [Technical Information Service, AEC] . 1949.
22. White, G. R. Gamma ray attenuation coefficients from 10 kev to 100 Mev. Nat. Bur. Standards Circular 583. 1957.



## VII. ACKNOWLEDGMENTS

I would like to express my gratitude to Dr. A. F. Veigt for his advice and encouragement during the course of this investigation.

My thanks also to Captain W. M. Drane, USN, Professor of Naval Science, and to the officers and men of the Naval Reserve Officers Training Corps for their valuable support during my studies at Iowa State College.

Finally, I would like to express my appreciation to the United States Navy for the opportunity to obtain an advanced technical education at the U. S. Naval Postgraduate School and Iowa State College.